

Supplementary data

Optimized local synthetic conditions induce size reduction and phase purification in $\{[\text{Fe}(\text{Htrz})_2(\text{trz})](\text{BF}_4)\}_n$ spin crossover particles

Tristan CASTEL^a, Anaïs MARCHETTI^b, Félix HOUARD^a, Nathalie DARO^b, Mathieu MARCHIVIE^b, Guillaume CHASTANET^{b,}, Kevin BERNOT^{a,c,*}.*

a) Univ. Rennes, INSA Rennes, CNRS, ISCR (Institut des Sciences Chimiques de Rennes), UMR 6226, F-35000 Rennes, FRANCE.

b) Univ. Bordeaux, CNRS, Bordeaux-INP, ICMCB, UMR 5026, F-33600 Pessac, FRANCE

c) Institut Universitaire de France, 1 rue Descartes, 75005, Paris, FRANCE

Figure SI1: Electron microscopy images of compounds 2a-c .	2
Figure SI2-5: DLS data analyses	3
Table SI1: Characteristic parameters extracted from DLS analyses	4
Figure SI6: Powder X-ray diffraction patterns of compounds 2a-c .	5
Figure SI7: Magnetic properties of compounds 2a-c .	6

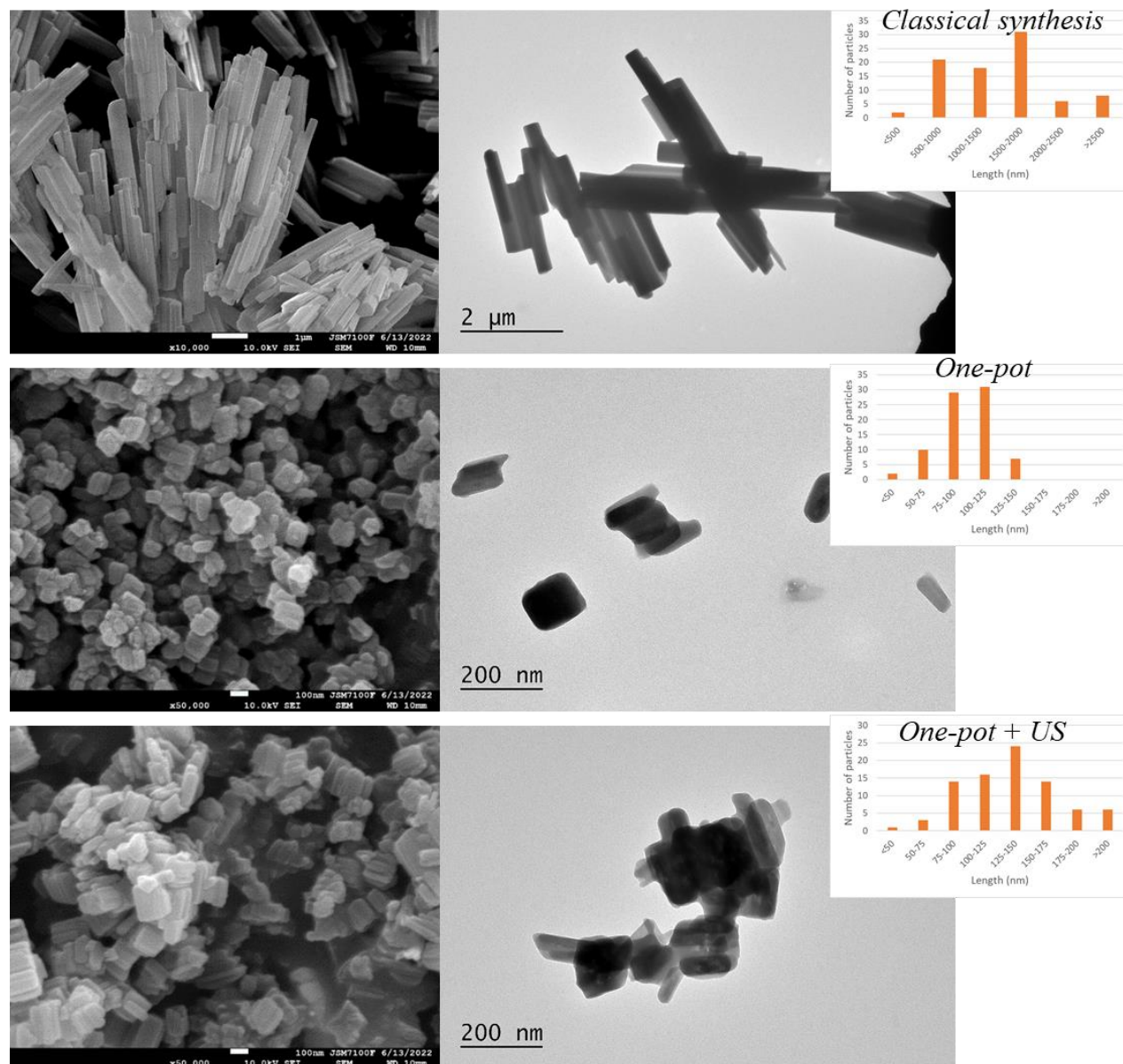


Figure S11. SEM (left, x 5k or 50k) and TEM (right) images of samples **2a** (top), **2b** (center), **2c** (bottom) with their respective length size distributions obtained from TEM analyses over more than 60 particles (inset).

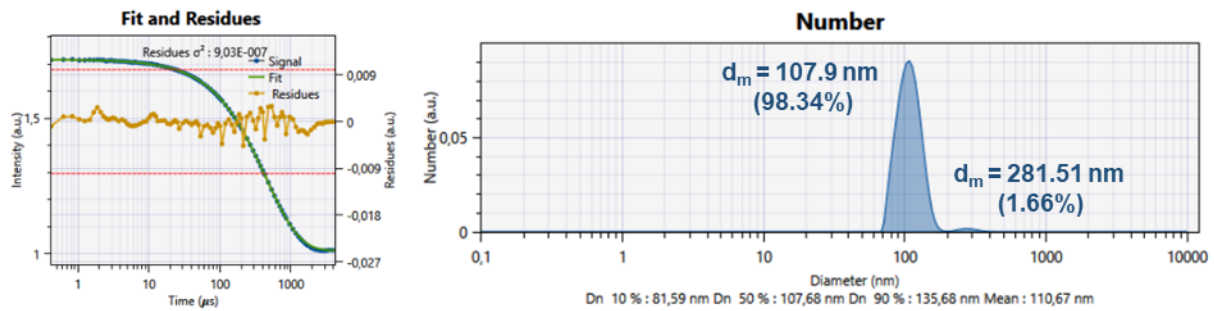


Figure SI2. Left: Correlogram of **1b** (dotted blue curve) with best fit (green curve) and corresponding residues (dotted orange curve). Right: Corresponding distribution size in number.

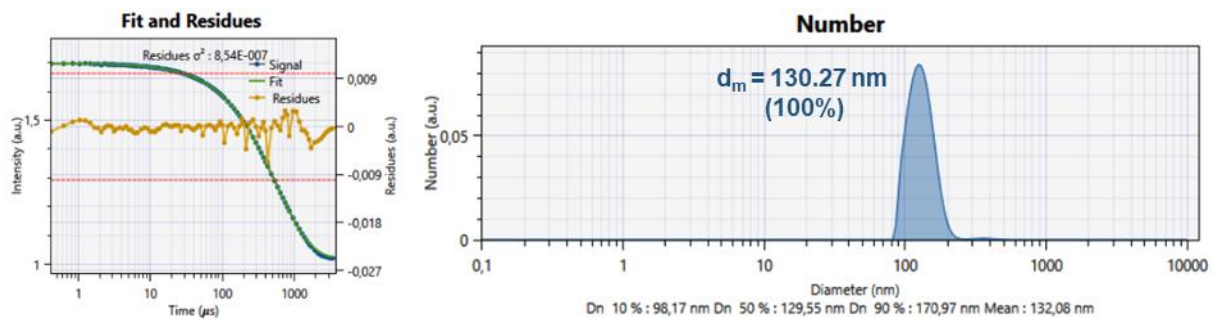


Figure SI3. Left: Correlogram of **1c** (dotted blue curve) with best fit (green curve) and corresponding residues (dotted orange curve). Right: Corresponding distribution size in number.

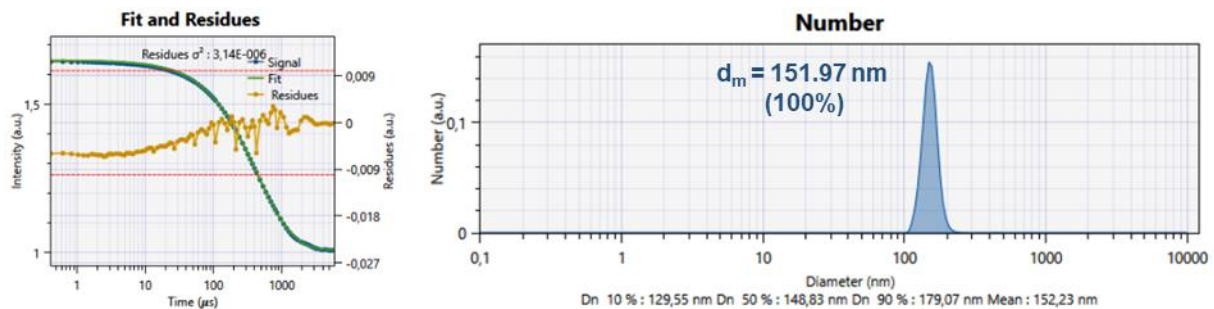


Figure SI4. Left: Correlogram of **2b** (dotted blue curve) with best fit (green curve) and corresponding residues (dotted orange curve). Right: Corresponding distribution size in number.

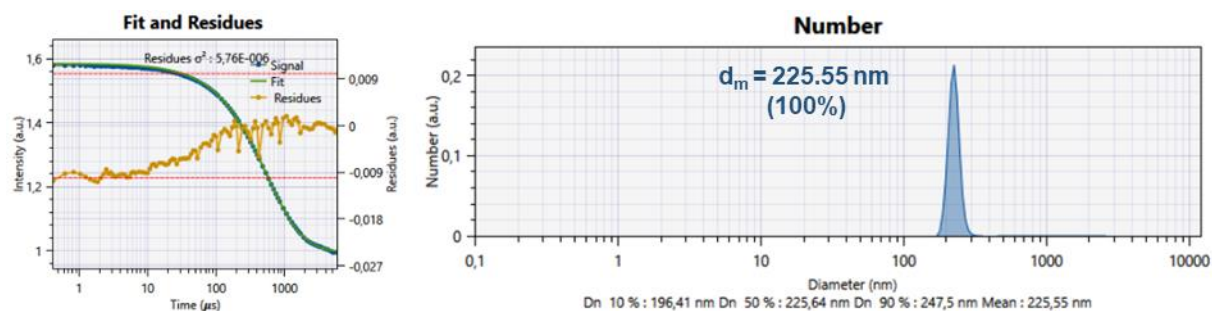


Figure SI5. Left: Correlogram of **2c** (dotted blue curve) with best fit (green curve) and corresponding residues (dotted orange curve). Right: Corresponding distribution size in number.

Table SI1. Characteristic parameters extracted from the above correlograms extracted with continuous multimodal Sparse Bayesian Learning (SBL) algorithm (in number) provided by the Nano Kin™ software (Cordouan Technologies, Pessac, France).

	Mode (nm)	Mean (nm)	Std Dev (%)	Number (%)	Decay Rate (s⁻¹)	Diffusion Coeff. (m²/s)
1b	107.68	107.9	18.91	98.34	2741.05	38.36525 E-13
	271.48	281.51	17.38	1.66	1087.22	15.21709 E-13
1c	123.7	130.27	20.84	100	2388.03	33.3962 E-13
2b	148.83	151.97	13.04	100	1983.15	27.75721 E-13
2c	225.64	225.55	9.68	100	138.07	18.3085 E-13

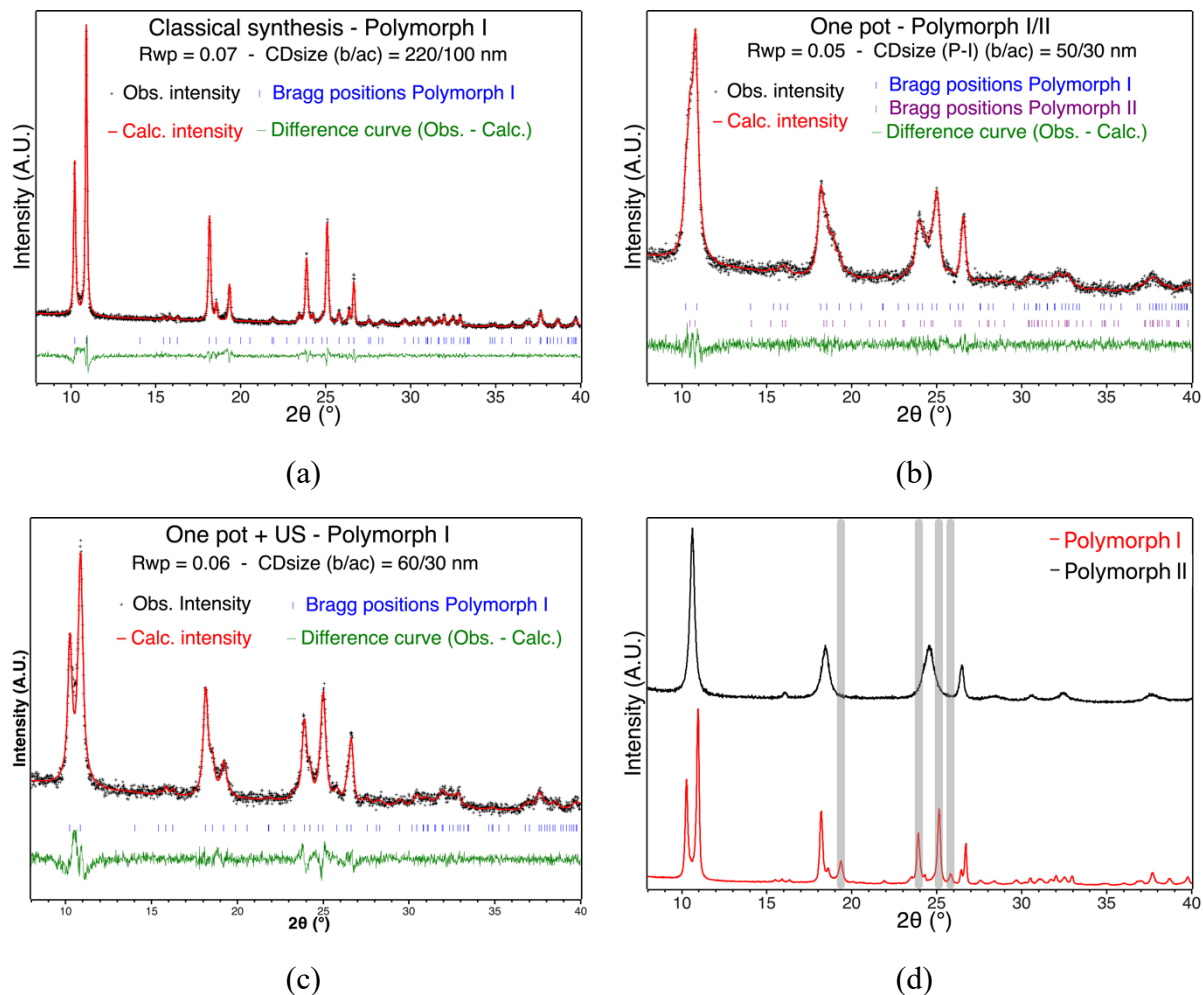


Figure S6. PXRD pattern for samples (a) **2a**, (b) **2b**, (c) **2c** with profile matching refinement (Le Bail) and theoretical peak positions of phases **I** and **II**. Peak broadening can be unambiguously assigned to a size reduction and a phase impurity (“one-pot”) or a size reduction only “one-pot + US”) on the basis of the refinement. Figure (d) shows the PDRX diagrams of pure polymorphs **I** and **II** showing some specific peaks of polymorph **I** (grey bands).

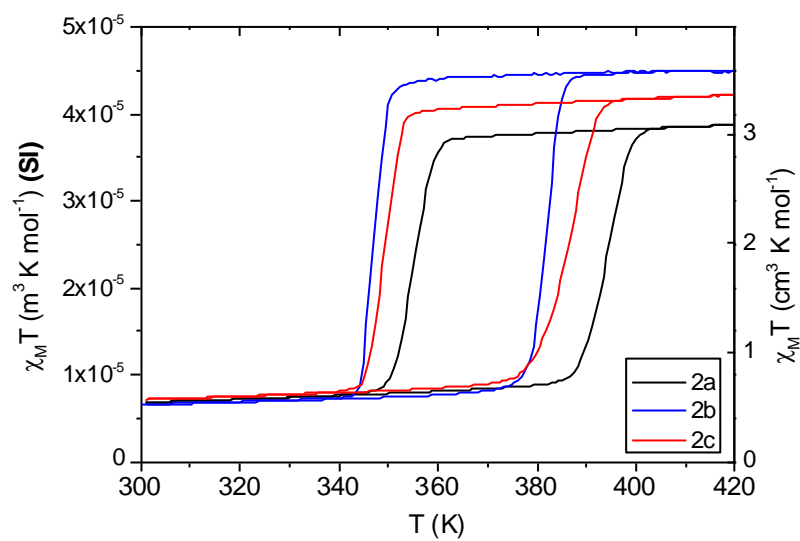


Figure SI7. Thermal evolution of the molar magnetic susceptibility χ_M times the temperature for **2a** (black curve), **2b** (blue curve) and **2c** (red curve). These curves correspond to the 4th cycle.